NAP-2023

IEEE International Conference "Nanomaterials: Applications & Properties"

Bratislava, SLOVAKIA, Sep. 10-15, 2023

Indexed by **Scopus**

CALL FOR PAPERS

MAIN TOPICS: ● Synthesis & Nanofabrication; ● Multifunctional Films & Coatings; ● Electrochemistry; ● Carbon-based Nanomaterials; ● Nanoscale Characterization; ● Electronic, Photonic & Quantum Materials & Properties; ● Magnetism, Magnetic Materials & Phenomena; ● Sensors & Nanodevices; Nanotechnology for Energy, Water & Environ. Applications; ● Nanomedicine & Bionanotechnology; ● Theory & Modeling.

CONFERENCE VENUE

Crowne Plaza Bratislava Hotel, https://cpbratislava.sk/
a four-star hotel on the historical city center in Bratislava

EARLY REGISTRATION FEES (*)

Regular attendees: 400 EUR / 400 USD
Ph.D. Students: 200 EUR / 200 USD
* before June 15th, 2023
Invited Speakers, IEEE Members: 20% discount

IMPORTANT DATES

Abstract Submission:	Feb. 01 - Apr. 15, 2023
4-Pages Paper Submission:	Apr. 15 - May 15, 2023
Early registration fees deadline:	June 15, 2023
Program posted online:	Aug. 15, 2023
On-site Registration	Sept. 10, 2023

CONFERENCE FORMAT & PRESENTATION

The plenary presentations are 40 min (+5min for Q&A)
The invited presentations are 25 min (+5min for Q&A)
The contribution talks are 10 min (+5min for Q&A)
Format for poster presentation is A0, portrait
Some onsite IEEE NAP-2023 events will be live streaming.

AWARDS & GRANTS

Rising Star in Nanoscience & Nanotechnology
Best Paper Award
"Nanoscience as Art" Competition
"East Meets West" Grant Program

ORGANIZING COMMITTEE

Honorary Chair: Pavol Šajgalík
General Chairs &
Local Organizing Committee Chairs:
Vladimír Cambel & Ľubomír Čaplovič
General Co-Chair: Alexander Pogrebnjak
Conference Secretary: Yurii Shabelnyk
Publication Chair: Oleksandr Prokopenko
Finance & Exhibits Co-Chairs: Valentine Novosad
& Miroslava Blázyová

Technical Program Committee: Goran Karapetrov (Chair), Andrii Chumak, Sorin Cotofana, Maksym Pogorielov, Milan Ťapajna, Viera Skakalova, Emerson Coy, Milan Sýkora, Oleksandr Dobrovolskiy, Ján Šoltýs
WiSE Co-Chairs: Michaela Sojková & Alina Dvornichenko
Awards & Grants Co-Chairs: Anna Marchenko & Martin Hulman
Student & YP Activities Co-Chairs: Kateryna Smyrnova, Matteo Bruno Lodi, Martin Sahul

🌐 *https://ieeenap.org*
✉ *info@ieeenap.org*

f *https://www.facebook.com/nap.conference*
in *https://www.linkedin.com/groups/4112736*

NAP-2023

Tracks & Topics

1. Nanomaterials Synthesis & Self-assembly

✓ Novel routes for synthesis of "building blocks";
✓ Size-, shape- and composition-dependent properties;
✓ Top-down and bottom-up approached for self-assembly;
✓ Block-co-polymers, interfacial science and morphology control; ✓ Nanocomposites & nanohybrids; ✓ 2D transition metal carbides/nitrides: MXenes.; ✓ Nano- and micro-fabrication techniques.

2. Multifunctional Thin Films & Coatings

✓ Advances in PVD, CVD and ALD techniques; ✓ Thin film growth & epitaxy; ✓ New thin film materials: diamond-like films, granular alloys, HEA, oxynitrides, intermetallic compounds; ✓ Hard, wear-, oxidation-resistant and multifunctional coatings; ✓ Electroplating and electroless deposition; ✓ Surface oxidation and corrosion properties; ✓ Industrial applications.

3. Electrochemistry of Nanomaterials

✓ Electrochemical processes at a nanoscale;   ✓ Nanomaterials and nanodevices for electrochemical sensing; ✓ Synthesis and characterization of electrocatalytic electrodes; ✓ Electrochemical surface modification and corrosion mechanisms; ✓ Photoelectrochemistry of nanomaterials; ✓ Electrochemical phenomena at the nanobio hybrids and interfaces.

4. Nanoscale Characterization & Imaging

✓ Optical, scanning probe, X-ray, ion- and electron microscopy;   ✓ Nanoscale science and engineering, including manipulation of matter at the atomic/molecular scale and assembly phenomena; ✓ Interactions at surfaces of soft matter, including polymers and biomaterials; ✓ Electrochemistry at surfaces and interfaces.

5. Nanophotonics

✓ Plasmonic structures and quantum dots; ✓ Near field microscopy; ✓ Nano-optics and optical tweezers; ✓ Spectroscopic studies of nanoscale materials; ✓ Molecular energy transfer and light harvesting; ✓ Photonic and optoelectronic materials and devices; ✓ Photo-detectors, sensors and imaging.

6. Transport Properties in Nanoscale Systems

✓ Molecular scale electronics; ✓ Transport properties in 2D materials; ✓ Nanocircuitry and nanowires; ✓ Heterostructures and quantum wells; ✓ Thermal transport and heat exchange at nanoscale.

7. Nanomagnetism & Magnetic Materials

✓ Magnetic nanoparticles, nanowires, thin films and patterned nanostructures; ✓ Magnetization reversal, domain structure, spin vortices and skyrmions; ✓ Spin waves and magnonics; ✓ Spin currents: generation, manipulation and transport; ✓ Spintronics: memories, field sensors, logic and spin-based devices; ✓ Magnetic anisotropy and recording media; ✓Heusler alloys, magnetocaloric and magneto-optical materials.

8. Superconductivity in Nanoscale & Mesoscopic Systems

✓Superconducting materials, thin films and patterned structures; ✓ Hybrid systems, proximity and size-dependent effects; ✓ Imaging and vortex dynamics; ✓ Josephson juncthions and nanoSQUIDs; ✓ Superconducting electronics, detectors and sensors.

9. Nanosensors & Nanodevices

✓ Field-effect transistors;   ✓ Micro/nano electromechanical systems and sensors; ✓ Piezoelectric sensors; ✓ Plasmonic and surface-enhanced Raman spectroscopy; ✓ Magnetoelectronic or spintronic nanodevices; ✓ RF, microwave, IR, UV-VIS and X-ray sensors, and single photon detectors; ✓ Quantum computing devices.

10. Nanomaterials for Energy & Environment

✓Nanomaterials for solar-to-electric energy conversion; ✓ Hydrogen and fuel cells; ✓ Energy storage and generation; ✓ Bio-inspired energy materials; ✓Nanomaterials for circular economy, environmental protection and remediation; CO reduction; ✓ Nanotech for water technologies.

11. Nanobiomedical Research & Applications

✓ Nanoparticles manipulation, microfluidics and lab-on-chip technologies; ✓Nanoplatforms for cancer diagnostics, imaging and treatment; ✓ Nanodevices and sensors for bio/nanomedicine; ✓ Bio-nanomaterials and tissue engineering; ✓ DNA nanotechnology; ✓ Nanotoxicity.

12. Theory & Modeling

✓First-principles methods; ✓ Non-equilibrium thermodynamics; ✓ Multiscale methods for charge/heat transport in nano- and mesoscale systems; ✓ Atomistic quantum transport simulations; ✓ Simulation of organic semiconductor devices; ✓ Microstructure-based models and dislocation analysis; ✓ Quantum computing.

Find more at:
https://ieeenap.org/topics

https://ieeenap.org
info@ieeenap.org
https://www.facebook.com/nap.conference
https://www.linkedin.com/groups/4112736

Synthesis of functional nanocomposites and nanohybrids based on the nanoscale oxide materials

Anatolii Belous[1] *, Ivan Lisovskyi[1], Pavlo Torchyniuk[1], Yuliia Shlapa[1]

[1] V. I. Vernadsky Institute of General & Inorganic Chemistry, NAS of Ukraine

(Ukraine)

* agbilous@ukr.net

Nanocomposites and nanohybrids have been attracting significant scientific and practical interest due to the possibility of combining various useful properties in one material and increasing its functionality. Such systems can find practical application both in technology (magnetic recording systems, elements of microwave technology, electrochemical systems) and in medicine (MRI, hyperthermia, drugs delivery). The synthesis of non-agglomerated or weakly agglomerated nanoparticles and the development of special-purpose nanocomposites based on them is a serious scientific task. The preparation of such composites depends essentially on the chemical composition of nanoparticles, their crystalline structure and physical-chemical properties, as well as on the method of synthesis.

The aim of this work was the synthesis of weakly agglomerated nanoparticles of various materials, in particular, ferrites based on complex oxide systems with spinel, perovskite, and barium hexaferrite structures; lithium-conducting systems with NASICON, perovskite and garnet structures, and also organic-inorganic perovskites. Such methods as precipitation in aqueous and non-aqueous solutions, inverse microemulsion, sol-gel, and spin-coating were used for the synthesis of materials. The relationships between the chemical composition, crystalline structure, and conditions of synthesis of weakly agglomerated nanoparticles were established. Synthesized nanoparticles were used to prepare functional nanohybrid materials for various purposes (hybrid magnetic films for microwave resonators, lithium-conductive films for lithium-ion batteries, organic-inorganic perovskites films for solar cells), and also nanocomposites with core/shell structure. Optimal methods for manufacturing structured nanocomposite and nanohybrid materials with controlled physical-chemical parameters were established. It has been shown that the synthesized composite materials possess an increased functional effect compared to existing nanoparticles. These composite materials can be used for the fabrication of controlled microwave resonant elements, for the development of electrochemical and photovoltaic systems, and also for medical and biological purposes.

Keywords: nanocomposites; synthesis; magnetic materials; lithium-conducting systems; organic-inorganic perovskite

Synthesis of Functional Nanocomposites and Nanohybrids Based on the Nanoscale Oxide Materials

A. Belous, I. Lisovskyi, P. Torchyniuk, Yu. Shlapa
V. I. Vernadsky Institute of General & Inorganic Chemistry
NAS of Ukraine
Palladina ave. 32/34, 03142 Kyiv, Ukraine
belous@ionc.kiev.ua

Abstract — **This work is devoted to the synthesis of nano-sized weakly agglomerated particles of materials with the structures of spinel, perovskite, barium hexaferrite, NASICON, and composites based on them. It was shown that the fabricated nanoparticles could be used to synthesize magnetic films and surface modification of cathode materials for electrochemical systems.**

Keywords — weakly agglomerated nanoparticles, nanocomposites, functional materials, magnetic materials, electrochemical systems.

I. INTRODUCTION

Nanocomposites and nanohybrids are of considerable scientific and practical interest due to the possibility of combining various beneficial properties in one material and increasing its functionality [1]. To create them, nanoparticles based on oxide systems, which are characterized by various properties, are often used. Such systems can find practical application both in engineering (magnetic recording systems [2], elements of microwave technology, improving the properties of electrochemical systems [3, 4]) and in medicine (MRI [5], hyperthermia [6, 7], delivery drugs [8]). For practical use, nanoparticles characterized by low agglomeration are needed. The synthesis of non-agglomerated or weakly agglomerated nanoparticles and creating the special-purpose nanocomposites based on them is a complex scientific task.

Fabrication of weakly agglomerated particles significantly depends on the chemical composition of nanoparticles, their crystal structure, physical-chemical properties, and on the method of synthesis. Synthesis in solutions is usually used for obtaining the nanoparticles of oxide systems. In the first stage of synthesis, amorphous precipitates are often formed, which at heat treatment at a high-temperature form highly-agglomerated crystalline precipitate. It can lead to high agglomeration and require significant mechanical grinding. Strongly agglomerated nanoparticles cannot be used in practice.

The purpose of this work was to find ways to synthesize weakly agglomerated nanoparticles of various materials, in particular, ferrites based on complex oxide systems with the structure of spinel, perovskite, and barium hexaferrite, lithium-conductive material with the NASICON structure, as well as the development of polycrystalline films for magnetic recording systems based on synthesized magnetic nanoparticles and improving the characteristics of cathode materials for lithium-ion batteries (LIBs) by applying a protective layer of nanoparticles of lithium-conductive material to their surface.

II. EXPERIMENTAL DETAILS

A. Synthesis of barium hexaferrite nanoparticles by precipitation from aqueous solutions

The starting powders were obtained by the co-precipitation method at pH=9 and by the sequential precipitation when $BaCO_3$ was precipitated at pH=9 on preliminary obtained iron (III) hydroxide at pH=4-4.5.

B. Synthesis of barium hexaferrite nanoparticles by the sol-gel method.

The initial sol-gel precursors were obtained by the Pechini method. $Ba(NO_3)_2$, $Fe(NO_3)_3 \cdot 9H_2O$, citric acid (CA), ethylene glycol (EG), and ammonia solution were used as starting reagents. The amount of EG was varied within the ratios (mol.) CA/EG == 1/3, 1/4, and 1/5 at pH 8. The obtained powders were calcined in the temperature range of 920-1470 K for 2 hours.

C. Synthesis of $La_{1-x}Sr_xMnO_3$ nanoparticles by sol-gel method

$La_{1-x}Sr_xMnO_3$ ($0.23 \leq x \leq 0.25$) (LSMO) nanoparticles were fabricated by the Pechini method. The aqueous solutions of metal nitrate salts $La(NO_3)_3$, $Sr(NO_3)_2$, and $Mn(NO_3)_2$ were the starting reagents for obtaining the precursor; citric acid (CA) and ethylene glycol (EG) were used as the gelling agents. To obtain $La_{1-x}Sr_xMnO_3$ crystalline nanoparticles (x = 0.23–0.25), which have magnetic properties, heat treatment of the precursor was performed in the temperature range of 673–1173 K.

D. Synthesis of Nanoparticles of $Ni_{1-x}Zn_xFe_2O_4$ (x = 0 – 1) materials with a spinel structure by precipitation from aqueous solutions

$Ni_{1-x}Zn_xFe_2O_4$ nanopowders with x = 0; 0.25; 0.50; 0.75; 0.80; 0.85; 0.90; 0.95 and 1.00 were synthesized by the precipitation method. Aqueous solutions of $Ni(NO_3)_2$, $Zn(NO_3)_2$, and $Fe(NO_3)_3$ were used as starting materials. Sodium hydroxide NaOH was used as a precipitant. At the

final stage, the obtained products were subjected to heat treatment in air at 1073 K for 2 hours.

E. Synthesis of $Li_{1.3}Al_{0.3}Ti_{1.7}(PO_4)_3$ nanoparticles by the sol-gel method.

$Li_{1.3}Al_{0.3}Ti_{1.7}(PO_4)_3$ (LATP) nanoparticles were synthesized by the sol-gel method. Li_2CO_3, an aqueous solution of $Al(NO_3)_3$, $C_{16}H_{28}O_6Ti$ (~75% in isopropanol), 85% H_3PO_4, 65% HNO_3, 25% NH_4OH, citric acid (CA), and ethylene glycol (EG) were used as starting reagents for the synthesis. To form the crystalline structure of the particles, heat treatment of the pyrolysis product (LATP precursor) was performed at a temperature of 1023 K for 2 hours.

F. Application of a protective layer of $Li_{1.3}Al_{0.3}Ti_{1.7}(PO_4)_3$ on the particles of the cathode material.

A commercial sample of $LiNi_{0.4}Co_{0.2}Mn_{0.4}O_2$ (hereinafter NMC 424), produced by MTI Co, was used as the cathode material [9]. The protective layer of LATP on the surface of particles of cathode material NMC 424 was formed using two methods – mechanical mixing and sol-gel technology [10]. For deposition of the LATP protective layer by mechanical mixing, the pure particles of the commercial cathode material NMC 424 and previously synthesized LATP nanoparticles were homogenized in isopropyl alcohol for 24 hours by an alternating stirring on a magnetic stirrer and ultrasonic homogenization. The obtaining suspension was dried to remove the solvent and was subjected to heat treatment at 1023 K for 2 hours at a heating rate of 5°/min. NMC 424 particles were added into the jar, where the LATP synthesis was carried out at the final stage of the synthesis to deposit a protective layer of LATP on the cathode material particles via the sol-gel method. LATP nanoparticles and cathode material were taken in the ratio of 1:99 wt. % [11].

The studied samples were marked:
• NMC 424 without LATP protective layer (pristine);
• NMC 424 with LATP protective layer applied by mechanical method (NMC_m);
• NMC 424 with LATP protective layer applied by the sol-gel method ($NMC_{sol-gel}$).

G. Method of analysis

The structural properties of the synthesized magnetic and lithium-conducting nanoparticles were studied using X-ray phase analysis (XRD) on a DRON-4 diffractometer (CuKα radiation, a step of 0.02°, a count time of 10s). The JCPDS database was used to analyze the XRD results. The morphology of the powders was observed using JEM 1230 / JEM 1400 transmission electron microscopes (Jeol, Japan) and FEG-SEM Nova Nanosem 230 FEI / SEC miniSEM SNE 4500 MB scanning electron microscope.

Magnetic measurements of the films were performed in a vibrating magnetometer (VSM, MLVSM9 MagLab 9 T, Oxford instrument) in parallel and perpendicular magnetic fields.

The charge/discharge characteristics of the LIB models were obtained using multichannel potentiostats ARBIN (MITS Pro Software of MSTAT 32, Arbin Corporation, USA) and VMP3 (Bio-Logic-Science Instruments, France).

III. RESULTS AND DISCUSSION

At the synthesis of nanoparticles of barium hexaferrite ($BaFe_{12}O_{19}$) by precipitation from aqueous solutions, when all components are simultaneously precipitated at pH ~ 9, amorphous precipitates are obtained. During heat treatment at a temperature ≥ 1270 K amorphous precipitates become highly agglomerated crystalline precipitates. Another situation is observed when the deposition is carried out in two stages. In the first stage, iron hydroxide ($Fe(OH)_3$) was deposited at pH ~ 4–4.5, and in the second stage, barium carbonate ($BaCO_3$) was deposited on the iron hydroxide precipitate at pH ~ 9. Soft precipitates with dimensions of 60–65 nm are formed after high-temperature treatment. (Fig. 1a).

At the synthesis of barium hexaferrite ($BaFe_{12}O_{19}$) nanoparticles by the sol-gel method after heat treatment at 570 K, a mixture of γ-Fe_2O_3, $BaCO_3$, and α-Fe_2O_3 phases is formed. It should be noted that the CA/EG ratio strongly affects the shape of nanoparticles after high-temperature treatment. The morphology of the sample obtained during heat treatment of the precursor (CA/EG = 1/3) has the lamellar shape of nanoparticles with d_{av} = 65 nm. The morphology of the sample with CA/EG = 1/4 is represented by nanoparticles in the form of plates (d_{av}= 70 nm) and rods (d_{av} = 40 nm, l_{av} = 90 nm). When the CA/EG ratio is 1/5, the sample is characterized by the formation of nanoparticles in the form of nanorods (d_{av} = 30 nm, l_{av} = 70 nm) (Fig. 1b).
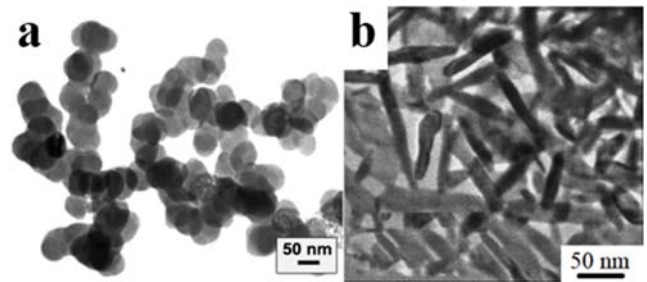

Fig. 1. TEM image of $BaFe_{12}O_{19}$ samples, obtained by **(a)** sequential precipitation and **(b)** sol-gel method after calcination.

At the synthesis of $La_{1-x}Sr_xMnO_3$ ($0.23 \leq x \leq 0.25$) by sol-gel method, the manganite nanoparticle was obtained after pyrolysis of the polyester formed during the polyesterification reaction between citric acid and ethylene glycol. The obtained TEM results indicate that the average diameter of the particles is 20–40 nm (Fig. 2). According to the literature, the average size of single-domain nanoparticles for manganite is about 70 nm [12]. The synthesized nanoparticles are single-domain, which is required for appearence of superparamagnetic properties.
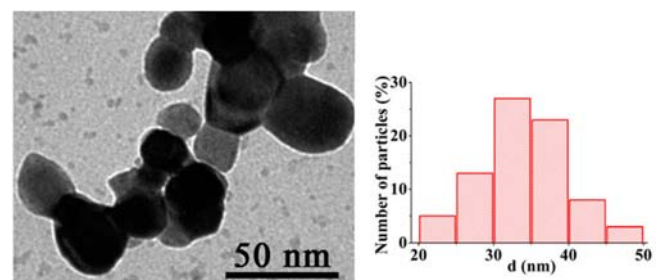
Fig. 2 TEM images and particle size distributions of LSMO nanoparticles synthesized via sol-gel method.

At the synthesis of $Ni_{1-x}Zn_xFe_2O_4$ nanoparticles (x = 0 – 1) with a spinel structure by precipitation from aqueous solutions, the results of X-ray phase analysis (XRD) showed that all $Ni_{1-x}Zn_xFe_2O_4$ samples with x = 0; 0.25; 0.50; 0.75; 0.80; 0.85; 0.90; 0.95 and 1 are crystalline, single-phase and have a cubic spinel structure with space group Fd-3m. TEM images demonstrate that the synthesized nanoparticles are nanosized and weakly agglomerated (Fig. 3).
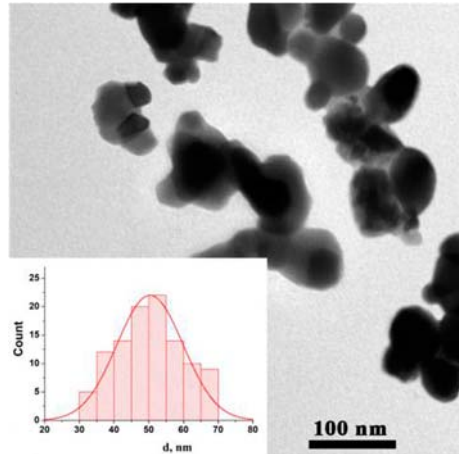
Fig. 3. TEM image of $Ni_{0.25}Zn_{0.75}Fe_2O_4$ nanoparticles. The inset shows a diagram of the size distribution of nanoparticles.

Field dependencies of mass magnetization (M) for $Ni_{1-x}Zn_xFe_2O_4$ samples (x = 0.25) are shown in Fig. 4. The magnetization of the sample $Ni_{1-x}Zn_xFe_2O_4$ (x = 0.25) reaches saturation when μ0 H exceeds ~ 300 mT.
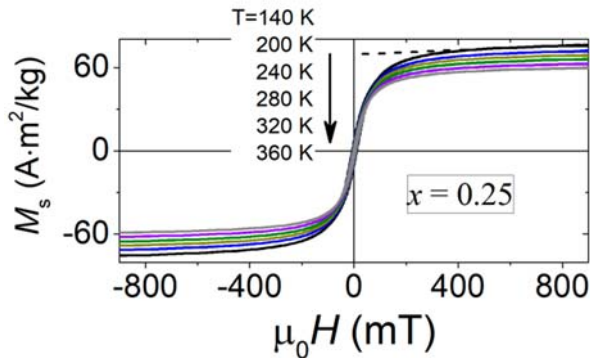

Fig. 4. Field dependences of mass magnetization for $Ni_{1-x}Zn_xFe_2O_4$ nanoparticles with x = 0.25. Dashed line illustrates the method of determination of spontaneous magnetization at a particular temperature.

Magnetic fluids were fabricated based on Ni1-xZnxFe2O4 nanoparticles and aqueous solutions of sodium oleate. It was established that the effect of an alternating magnetic field leads to the heating of nanoparticles. The heating efficiency decreases with increasing zinc content in the samples, which is very important for application of these materials in biology and medicine.

Barium hexaferrite nanoparticles with an anisotropic shape were used for preparing the polycrystalline films.

Polycrystalline films based on barium hexaferrite nanoparticles were obtained by sol-gel and spin-coating methods. Polished α-Al$_2$O$_3$ plates were used as a substrate.

Single-phase barium hexaferrite films were obtained in the temperature range of 1073–1173 K. EDX data showed that these films have a uniform distribution of barium and iron ions on the film's surface. According to the SEM results, the thickness of the film was 200 nm (Fig. 5a). The microstructure of the film is characterized by a rod-like particle shape (d_{av} = 62 nm, l_{av} = 320 nm, l_{av} / d_{av} =5) (Fig. 5b). The anisotropy of the particles' shape makes it possible to obtain highly efficient films for magnetic recording systems.
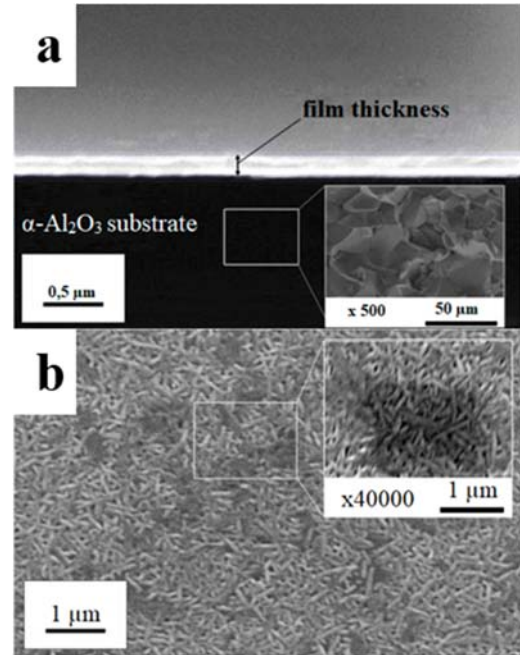

Fig. 5. SEM image of the (a) cross-section and of the surface the barium hexaferrite film after heat treatment at T = 1173 K.

For the barium hexaferrite films, the coercivity (H_c = 334.23 kA/m) and the saturation magnetization (M_s = 0.005 emu) were determined when the magnetic field was directed perpendicular to the film surface. These values are higher than similar values obtained when the magnetic field is oriented parallel to the plane of the film (H_c = 167.11 kA/m and M_s = 0.003 emu). It indicates a predominant perpendicular magnetic anisotropy in this film.

Effect of surface modification of commercial cathode materials on the electrochemical characteristics.

Fig. 6 shows the results of XRD analysis of pure cathode material NMC 424 and LATP nanoparticles synthesized by the sol-gel method (Fig. 6a), and cathode materials with a protective layer of LATP (1 wt. %) applied using two methods (Fig. 6b). The XRD results show that the cathode material has a hexagonal-layered structure of the α-NaFeO$_2$ type with space group R3m, which is confirmed by the splitting of the (006)/(012) peaks, and LATP has a rhombohedral structure with space group R-3c. The peaks of the NASICON rhombohedral structure are not observed in XRD patterns of cathode materials with a protective layer of LATP. It is

connected with the small thickness of the LATP protective layer on the surface of the particles of the cathode materials.
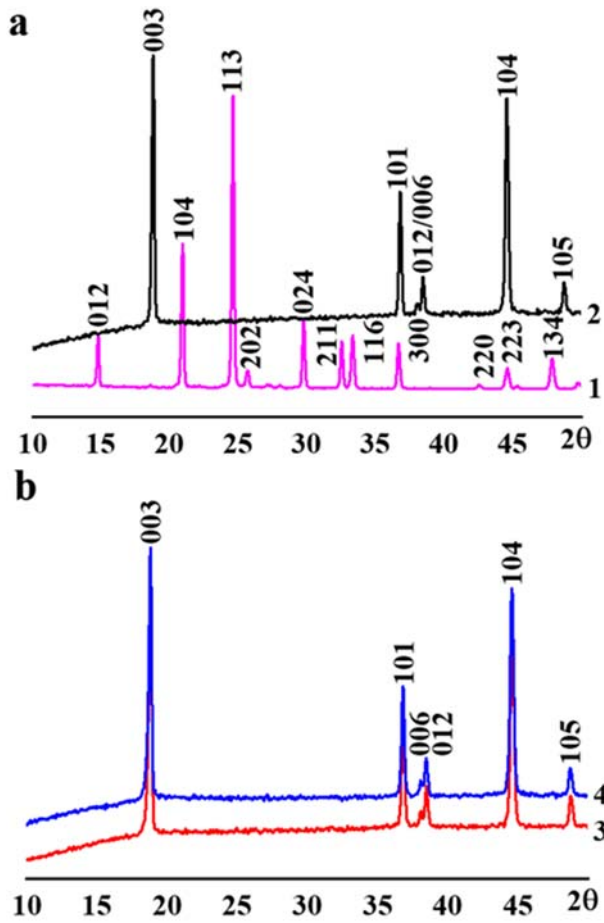

Fig. 6. XRD results of (a) LATP nanoparticles synthesized by the sol-gel method (1) and the pure cathode material NMC 424 (2); (b) cathode material coated with LATP protective layer using different methods: 1 – NMC$_{m}$; 2 – NMC$_{sol-gel}$.

The morphology of the pure NMC 424 cathode material and the cathode material with the LATP protective layer is shown in Fig.7. Particles of the pure cathode material have a spherical shape and dimensions of about 8 mm. The surface of the particles is porous, not homogeneous and consists of a large number of particles with a size about 200–500 nm. In contrast to the pure cathode material, many smaller particles are observed on the surface of NMC particles with a protective layer (Fig. 7b and 7c). The surface of NMC particles with a protective layer is more homogeneous.
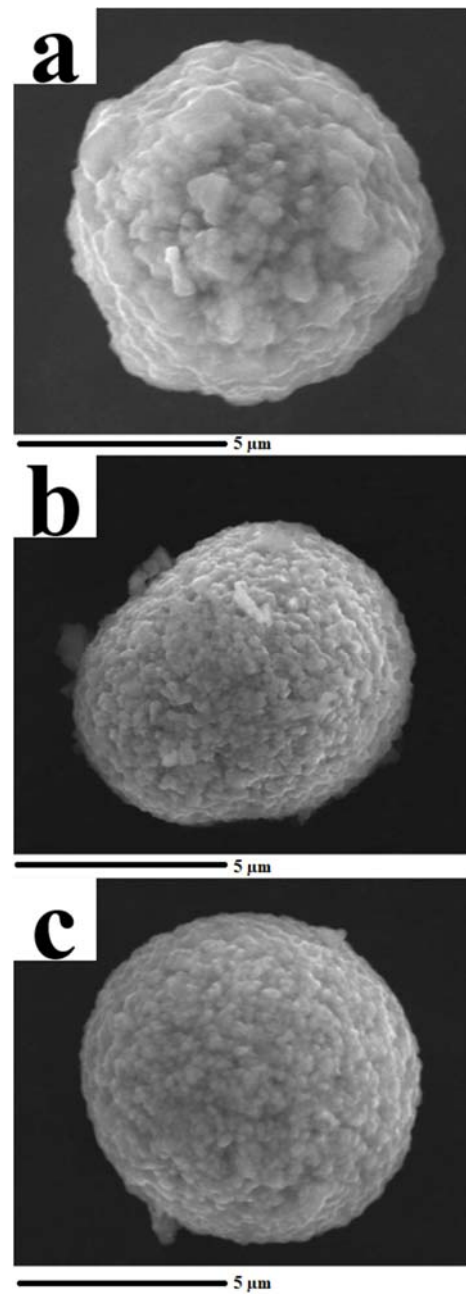
Fig. 7. SEM images of the pristine cathode material NMC 424 and LATP-coated cathode material using diferent methods: a – pristine NMC 424; b – NMC$_{m}$; c – NMC$_{sol-gel}$.

Fig. 8 shows the dependence of the specific capacity on the charge/discharge current density of the pure cathode material NMC 424 and cathode materials with a protective layer of LATP in the voltage range from 2.5 to 4.2 V. The capacity retention for cathode materials with a protective LATP coating is significantly higher than for the pure cathode material when the current density increases. For example, at a current density of 30C, the capacity retention of the pure cathode material is 30%, while for NMC$_{m}$ – 35%, and NMC$_{sol-gel}$ – 43%.
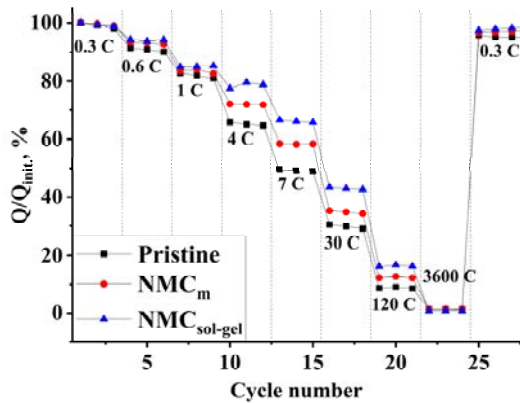
Fig. 8. Specific capacity of the pristine cathode material and cathode materials with a protective LATP layer at different current densities.

Fig. 9 shows the results of galvanostatic cycling of LIB models with cathodes based on the pristine NMC, NMC$_m$, and NMC$_{sol-gel}$ in the voltage range of 2.7–4.3 V. Cathode materials with a protective layer of LATP are characterized by both higher initial capacity and better stability of characteristics over a long-term charge/discharge cycling. The capacity drop at the 80th cycle for the pure cathode material is 8%, while this value is less than 1% for the modified samples.
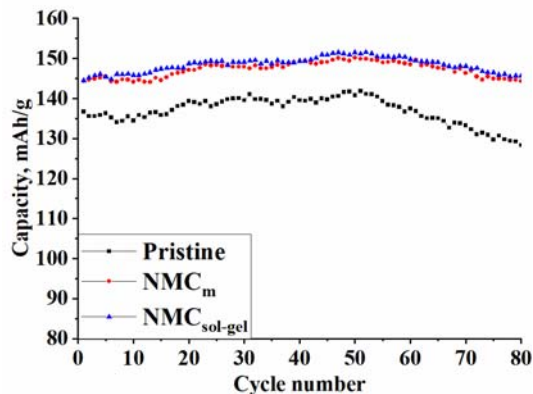

Fig. 9. Change in the specific capacity of the pristine NMC and cathode materials with a protective LATP layer during long-term charge/discharge cycling at a current density of C/5.

IV. Conclusion

This study defines the relationship between chemical composition, crystal structure, and synthesis conditions of weakly agglomerated nanoparticles. It has been shown the possibility of using synthesized nanoparticles for fabricating the nanocomposites for various purposes, namely, hybrid magnetic films and modified cathode materials for lithium-ion batteries. Optimal methods of creating structured nanocomposite and nanohybrid materials with controlled physicochemical parameters have been established. It was shown that the synthesized composite materials have an increased functional effect compared to individual materials based on the same nanoparticles. These composite materials can be used for the manufacture of controlled microwave resonant elements, for the development of electrochemical systems, as well as for medical and biological purposes.

References

[1] J. Kudr, Y. Haddad, L. Richter, Z. Heger, M. Cernak, V. Adam, and O. Zitka, "Magnetic nanoparticles: From design and synthesis to real world applications." Nanomaterials, vol. 7, № 9, p. 243, August 2017.

[2] S. B. Galvão, A. C. Lima, S. N. De Medeiros, J. M. Soares, and C. A. Paskocimas, "The effect of the morphology on the magnetic properties of barium hexaferrite synthesized by Pechini method.", Materials Letters, vol. 115, pp. 38–41, January 2014.

[3] S.-T. Myung, F. Maglia, K.-J. Park, C.S. Yoon, P. Lamp, S.-J. Kim, and Y.-K. Sun, "Nickel-rich layered cathode materials for automotive lithium-ion batteries: achievements and perspectives." ACS Energy Letters, vol. 2, pp.196–223, January 2017.

[4] S. Xia, F. Li, F. Chen, and H. Guo, "Preparation of FePO$_4$ by liquid-phase method and modification on the surface of LiNi$_{0.80}$Co$_{0.15}$Al$_{0.05}$O$_2$ cathode material." J. Alloys Compd., vol. 731, pp. 428–436, January 2018.

[5] A. Avasthi, C. Caro, E. Pozo-Torres, M. P. Leal, and M. L. García-Martín, "Magnetic nanoparticles as MRI contrast agents." in Surface-modified Nanobiomaterials for Electrochemical and Biomedicine Applications, A.R. Puente–Santiago and D. Rodriguez-Padron Eds., Springer, 2020, pp. 49–91.

[6] A. Farzin, S. A. Etesami, J. Quint, A. Memic, and A. Tamayol, "Magnetic nanoparticles in cancer therapy and diagnosis." Adv. Healthc. Mater., vol. 9, № 9, p.1901058, March 2020

[7] J. Jose, R. Kumar, S. Harilal, G. E. Mathew, D. G. T. Parambi, A. Prabhu, S. Uddin, L. Aleya, H. Kim, and B. Mathew, "Magnetic nanoparticles for hyperthermia in cancer treatment: an emerging tool." Environ. Sci. Pollut. Res., vol. 27, pp.19214–19225, December 2020.

[8] S. Mura, J. Nicolas, and P. Couvreur, "Stimuli-responsive nanocarriers for drug delivery." Nature materials, vol. 12, № 11, pp. 991–1003, October 2013.

[9] H.-J. Noh, S. Youn, C. S. Yoon, Y.-K. Sun, "Comparison of the structural and electrochemical properties of layered Li[Ni$_x$Co$_y$Mn$_z$]O$_2$ (x = 1/3, 0.5, 0.6, 0.7, 0.8 and 0.85) cathode material for lithium-ion batteries." J. Power Sources, vol. 233, pp. 121–130, July 2013.

[10] I. Lisovskyi, S. Solopan, A. Belous, V. Khomenko, and V. Barsukov, "An effective modification of LiNi$_{0.6}$Co$_{0.2}$Mn$_{0.2}$O$_2$ with Li$_{1.3}$Al$_{0.3}$Ti$_{1.7}$(PO$_4$)$_3$ as a high-performance cathode material for Li-ion batteries." J. Appl. Electrochem., vol. 52, № 12, pp. 1701-1713, July 2022.

[11] S. Kobylianska, D. Demchuk, V. Khomenko V. Barsukov, and A. Belous, "Surface Modification of the LiNi$_{0.5}$Co$_{0.2}$Mn$_{0.3}$O$_2$ Cathode by a Protective Interface Layer of Li$_{1.3}$Ti$_{1.7}$Al$_{0.3}$(PO$_4$)$_3$." J. Electrochem. Soc., vol. 166, № 10, p. A1920, June 2019.

[12] P. Dey, and T.K. Nath, "Tunable room temperature low-field spin polarized tunneling magnetoresistance of La$_{0.7}$Sr$_{0.3}$MnO$_3$ nanoparticles." Appl. Phys. Lett., vol. 89, p.163102, October 2006.

Manuscript review

Logs

№	Status	Date
1	Submitted	2023-06-02
2	In Review	2023-07-16